

This is the accepted manuscript made available via CHORUS. The article has been published as:

## Quantum oscillations in $\text{EuFe}_{\{2\}}\text{As}_{\{2\}}$ single crystals

P. F. S. Rosa, B. Zeng, C. Adriano, T. M. Garitezi, T. Grant, Z. Fisk, L. Balicas, M. D.

Johannes, R. R. Urbano, and P. G. Pagliuso

Phys. Rev. B **90**, 195146 — Published 24 November 2014

DOI: [10.1103/PhysRevB.90.195146](https://doi.org/10.1103/PhysRevB.90.195146)

# Quantum Oscillations in $\text{EuFe}_2\text{As}_2$ single crystals

P. F. S. Rosa,<sup>1,2</sup> B. Zeng,<sup>3</sup> C. Adriano,<sup>1</sup> T. M. Garitezi,<sup>1</sup> T. Grant,<sup>2</sup> Z. Fisk,<sup>2</sup> L. Balicas,<sup>3</sup> M. D. Johannes,<sup>4</sup> R. R. Urbano,<sup>1</sup> and P. G. Pagliuso<sup>1</sup>

<sup>1</sup>*Instituto de Física “Gleb Wataghin”, UNICAMP, Campinas-SP, 13083-859, Brazil.*

<sup>2</sup>*University of California, Irvine, California 92697-4574, USA.*

<sup>3</sup>*National High Magnetic Field Laboratory, Florida State University, Tallahassee, Florida 32310, USA.*

<sup>4</sup>*Center for Computational Materials Science, Code 6390, Naval Research Laboratory, Washington, DC 20375, USA.*

Quantum oscillation measurements provide relevant information about the Fermi surface (FS) properties of strongly correlated metals. Here, we report on the Shubnikov-de Haas (SdH) effect via high-field resistivity measurements of  $\text{EuFe}_2\text{As}_2$  (Eu122) and  $\text{BaFe}_2\text{As}_2$  (Ba122) single crystals. Although both pnictide compounds are isovalent with similar effective masses and density of states at the Fermi level, our results reveal subtle changes in their fermiology. Remarkably, although the spin-density-wave (SDW) ordering temperature is higher in the Eu-rich end, Eu122 displays a much more isotropic and 3D-like FS when compared with Ba122, in agreement with band structure calculations. Our experimental results suggest an anisotropic contribution of the Fe 3d orbitals to the FS in Ba122. We speculate that this orbital differentiation may be responsible for the suppression of the SDW phase in the FeAs-based compounds.

PACS numbers: 74.70.Xa, 71.18.+y

## I. INTRODUCTION

The Fe-based superconductors (SC) have been a subject of intensive investigation owing to their high superconducting transition temperature ( $T_c$ ) reaching values up to 56 K<sup>1-4</sup>. Although all members present FeAs layers as the common structural parameter, there is a variety of dissimilarities in their physical properties, such as magnetic ordered moments, effective masses, size of SC gaps and  $T_c$  itself<sup>5</sup>. For instance,  $\text{KFe}_2\text{As}_2$  is a non-magnetic metal which superconducts below 4 K while  $\text{BaFe}_2\text{As}_2$  (Ba122) undergoes a transition from a paramagnetic to a spin density wave (SDW) metallic state at 139 K, closely related to a structural transition<sup>6</sup>. Nonetheless, superconductivity can be induced in Ba122 by either hydrostatic pressure and/or chemical substitution (e.g. K, Co, Ni, Cu, and Ru). A deep understanding of such differences still remains an open question. In this regard, it is vital to unveil the Fermi surface (FS) geometry and symmetry, as well as the role of local distortions, given that they might be strongly related to the nature of the magnetic fluctuations in momentum space.

Experimentally, the most widely employed technique to directly access the electronic structure of crystals is angle resolved photoemission spectroscopy (ARPES). For the parent compounds  $A\text{Fe}_2\text{As}_2$  ( $A = \text{Ba}, \text{Ca}, \text{Eu}, \text{Sr}, \dots$ ), ARPES data usually display four Fe 3d FS sheets in the paramagnetic regime: two electron-like bands around the  $M$ -point and two hole-like bands around the  $\Gamma$ -point of the Brillouin zone (BZ). Furthermore, polarized ARPES measurements show the predominance of  $t_{2g}$  orbitals ( $xy$ ,  $xz/yz$ ) at the FS with the outer hole-pocket being mostly  $xy$ , in agreement with DFT + DMFT calculations<sup>10,12,14,15</sup>. Interestingly, a comparison between Ba122 and Eu122 in the paramagnetic state reveals that the outer hole  $xy$  pocket in Ba122 is half

the size of Eu122<sup>13</sup>, suggesting an increase of the planar  $xy$  occupation in the Ba-rich end. It is noteworthy that it is possible to change the occupation between distinct  $t_{2g}$ , or even  $e_g$ , orbitals although the total Fe occupation remains the same. Although such symmetry changes are carried to the FS, their precise influence is not fully understood yet. In addition, as the temperature is lowered below  $T_{\text{SDW}}$ , further striking consequences such as FS reconstruction, band splitting, opening of gaps, etc., are expected. Nonetheless, ARPES is a surface sensitive technique and it is highly desirable to confront its results with bulk FS experiments since the electronic structure on the surface may differ from the one in the bulk.

Within this context, the determination of a precise FS by a bulk-sensitive experimental technique is crucial and quantum oscillation (QO) measurements have been proven to be an important complementary technique to ARPES<sup>16,17</sup>. In particular, low temperature QO experiments have been reported on several members of the 122 family  $A\text{Fe}_2\text{As}_2$  ( $A = \text{Ba}, \text{Ca}, \text{Sr}$ ) providing both high resolution of the FS in momentum space and important information on the effective masses<sup>18-21</sup>. In particular, three low frequency Fourier peaks have been observed for  $\text{BaFe}_2\text{As}_2$  at  $F_\delta = 500$  T,  $F_\alpha = 440$  T, and  $F_\gamma = 90$  T, each of them occupying about 2% of the nonmagnetic BZ. However, up to date, no QO data have been reported for Eu122 although single crystals with residual resistivity ratio (RRR) as high as 15 have been synthesized<sup>22</sup>. The semi-metal  $\text{EuFe}_2\text{As}_2$  compound is unique because it displays both SDW phase transition at 190 K and antiferromagnetic phase transition at  $T_N = 19$  K due to the  $\text{Eu}^{2+}$  moments. Interestingly, Eu122 also undergoes a metamagnetic transition at  $H_m \sim 2$  T from a AFM state to a FM one. Thus, there is no additional reconstruction of the FS due to the long range ordering of the Eu moments at low temperatures.

In this paper, we report a comparative Shubnikov de-Haas (SdH) study between Eu122 and Ba122 single crystals grown by In-flux. Our results for Ba122 are in good agreement with previous reports<sup>18–20</sup> and the unprecedented observation of QO in Eu122 indicates that the Indium flux technique yields high quality single crystals. Subtle changes in the fermiology of Eu122, such as band splitting and a significant increase of isotropy and three-dimensionality of the bands, are clearly noticed when comparing the data with those of Ba122. Our main findings shed new light on the understanding of the SDW state and provide a possible scenario for the differences in the physical properties of this class of materials.

## II. EXPERIMENTAL DETAILS AND THEORETICAL METHODS

Single-crystalline samples of  $\text{EuFe}_2\text{As}_2$  were grown using the Indium flux technique with starting composition  $\text{Eu:Fe:As:In}=1:2:2:25$ . The mixture was placed in an alumina crucible and sealed in a quartz tube under vacuum. The sealed tube was heated up to  $1100^\circ\text{C}$  for 8 h and then cooled down to  $1000^\circ\text{C}$  at  $2^\circ\text{C/h}$ . The furnace was then turned off and the excess of In flux was removed at  $400^\circ\text{C}$  by centrifugation. Single-crystalline samples of  $\text{BaFe}_2\text{As}_2$  were grown as described in Ref.<sup>7</sup>. Our crystals were checked by X-ray powder diffraction and elemental analysis using a commercial Energy Dispersive Spectroscopy (EDS) microprobe. Specific-heat measurements were performed in commercial small-mass calorimeter that employs a quasiadiabatic thermal relaxation technique. The in-plane resistivity ( $\rho_{ab}(T)$ ) was measured using a standard four-probe method inside a  $^3\text{He}$  cryostat. Magnetic fields up to 35 T and 45 T were applied at the National High Magnetic Field Laboratory in Tallahassee, FL. The samples were discretely rotated between  $0^\circ$  and  $90^\circ$  with an in-plane rotation axis. Here,  $0^\circ$  stands for  $H$  parallel to the  $c$ -axis.

The theoretical Fermi surfaces were calculated using density functional theory with a full-potential augmented plane wave code, Wien2k<sup>23</sup>, using the local density approximation (LDA)<sup>24</sup> and its extension, LDA+U<sup>25</sup> to remove the localized Eu  $f$  states from the Fermi level ( $E_F$ ). The presented calculations employ an “U” value 8 eV and a “J” value of 1 eV, where  $J$  is the on-site exchange between electrons on a single Eu ion. Nevertheless, the electronic structure within several eV of  $E_F$  is insensitive to this particular choice. The experimental lattice parameters and atomic positions were extracted from Refs.<sup>26</sup> and<sup>27</sup> for the Eu and Ba based systems, respectively. We established the so-called magnetic “stripe” phase in which the basic unit cell is doubled both in-plane and along the  $c$ -axis to account for the anti-ferromagnetic ordering in both directions, resulting in an orthorhombic cell (space group 53). For the Eu compound, the Eu moments are aligned with each other in-plane and between planes, in agreement with the experimentally observed

ferromagnetic state at high fields<sup>28</sup>. We used a mesh of  $23 \times 23 \times 7$  kpts in the irreducible Brillouin zone.

## III. RESULTS AND DISCUSSION

Fig. 1 displays  $\rho_{ab}(T)$  at zero magnetic field for the studied compounds. A linear metallic behavior is observed down to  $T_{\text{SDW}}$  where a sudden drop is identified in the curves of Eu122 and Ba122 at 193 K and 139 K, respectively. The transition to a SDW state can also be seen as a sharp peak in the specific heat of both compounds (right hand side inset of Fig. 1). In addition, as the temperature is further decreased, a second drop is observed in Eu122 due to the  $\text{Eu}^{2+}$  AFM ordering at 19 K (left hand side inset to Fig. 1). Residual resistivity and RRR values for Eu122 are  $\rho_0 \simeq 10 \mu\Omega\cdot\text{cm}$  and  $\text{RRR} \simeq 25$ , respectively, indicating a high degree of crystallinity.

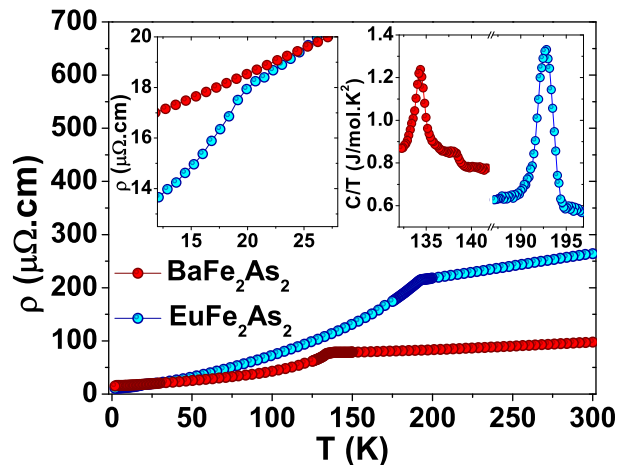


FIG. 1: Zero field in-plane resistivity  $\rho_{ab}(T)$  for Eu122 and Ba122 single crystals. The left hand side inset shows the  $\text{Eu}^{2+}$  AFM ordering temperature and the right hand side inset shows the SDW anomaly in the specific heat for both samples.

Figs. 2a and 2b show  $\rho_{ab}(T)$  at 0.3 K of our Eu122 and Ba122 single crystals as a function of applied magnetic field, respectively. After subtracting a smooth 4th order polynomial background, anisotropic QO are clearly observed above  $\sim 15$  T. The Fast Fourier Transform (FFT) of these QO as a function of frequency is presented in Figs. 2c and 2d. Four distinct low frequency peaks can be identified for both compounds. The corresponding frequencies are listed in Table I by adopting an identical labeling of the branches as in Ref.<sup>20</sup>. In particular, we also attribute the  $\beta$  branch reported in Ref.<sup>19</sup> to the second harmonic of the  $\gamma$ -orbit due to their similar angular dependency in both compounds. It is worth noting that, except for  $F_\delta$ , all other pockets are slightly smaller in Eu122, suggesting a subtle change of fermiology.

Remarkably, Eu122 presents a band splitting in the predominant  $\alpha$  pocket, in agreement with ARPES measurements below  $T_{\text{SDW}}$ <sup>10</sup>. In addition, combinations of

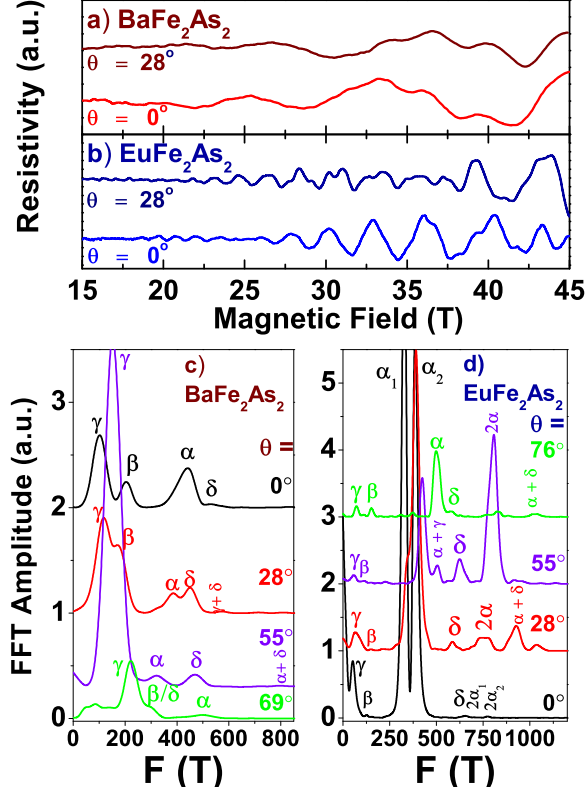


FIG. 2:  $\rho_{ab}(T)$  as a function of magnetic field for a)  $\text{EuFe}_2\text{As}_2$  and b)  $\text{BaFe}_2\text{As}_2$  single crystals at  $0^\circ$  and  $25^\circ$ , after subtracting a 4th order polynomial background. Here,  $0^\circ$  stands for  $H$  parallel to the  $c$ -axis. c) and d) are the Fast Fourier Transform (FFT) amplitude of the QO of the data in a) and b), respectively.

smaller orbits are observed at higher frequencies for both compounds, as reported previously in  $\text{Ba122}^{11}$ , although we were able to identify such frequencies more clearly in  $\text{Eu122}$ , likely due to its higher signal-to-noise ratio. In the present study, combination of frequencies can be ascribed to two main reasons. Firstly, magnetic interactions between carriers may give rise to nonlinear coupling of Fermi surface orbits and, ultimately, frequency mixing. In fact, the formation of the spin-density wave phase at low temperatures corroborates with this scenario. Nevertheless, combination of orbits may be also due to magnetic field-induced tunneling from one part of the FS to another, i.e., magnetic-breakdown orbits. An estimate of the breakdown field gives  $B \sim m^* E_g / \hbar e E_F \sim 18$  T, which is within our experimental range. Here,  $E_g \sim 190\text{K} \sim 16$  meV and  $E_F \sim 120$  meV extracted from the band structure calculations in Ref.<sup>19</sup>. However, we emphasize that such estimate assumes a separation between orbits in  $k$ -space of the order of this gap.

We now investigate how the observed frequencies evolve with temperature. Fast Fourier Transform (FFT) signal amplitudes with increasing temperature are shown in Fig. 3a for  $\text{Eu122}$ . The corresponding suppression of the SdH signal amplitude as a function of temperature

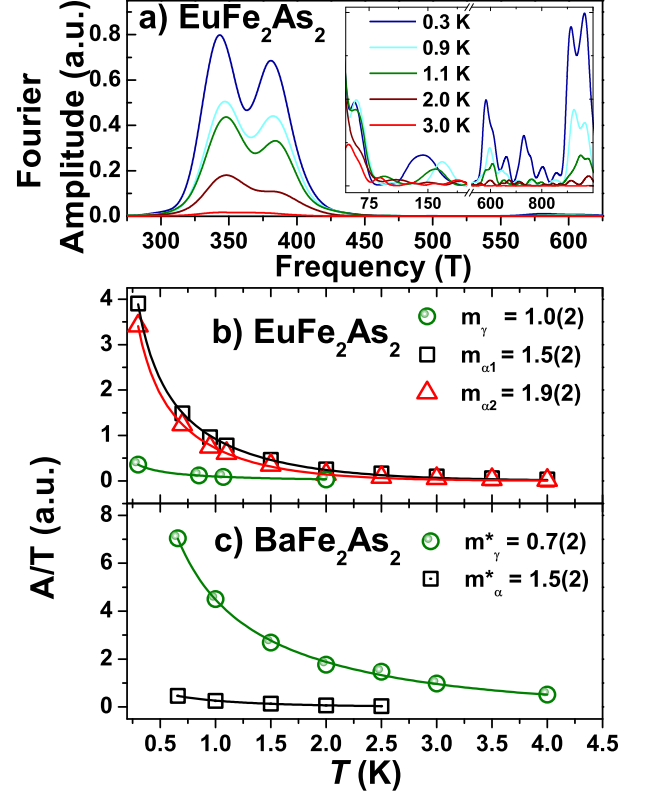


FIG. 3: a) FFT amplitude of the  $\text{Eu122}$  compound as a function of frequency for several temperatures. The inset displays less intense peaks. The FFT amplitude divided by temperature  $A/T$  as a function of temperature for b) the observed pockets of  $\text{Eu122}$  and, c) the observed pockets of  $\text{Ba122}$ .

is shown in Figs. 3b and 3c for  $\text{Eu122}$  and  $\text{Ba122}$ , respectively. Such suppression allows one to extract the corresponding effective masses by fitting  $A/T$  with the thermal damping term  $R_T = X/\sinh(X)$  of the Lifshitz-Kosevick (LK) formalism (solid lines in Fig. 3b-c), where  $X = 14.69 m^* T / B$  and  $m^*$  is the effective mass and  $1/B$  is the average inverse field of the Fourier window. Our analysis was not able to determine with accuracy the effective masses for  $\delta$  and  $\beta$  pockets in  $\text{Ba122}$ . Concerning the  $\delta$  pocket, the amplitude determination with increasing temperature is hindered by the lower signal-to-noise ratio due to a very weak FFT signal amplitude, as observed previously in ref.<sup>19</sup>. In the  $\beta$  pocket, the slight variation of position with temperature yield an inaccurate effective mass determination. Our results for the effective masses of  $\text{Ba122}$  and  $\text{Eu122}$  are shown in Table 1 and a comparison to the results obtained previously for  $\text{Ba122}$  is presented in Table II. Such comparison reveals that  $m^*$  is similar in  $\text{Ba122}$  and  $\text{Eu122}$  compounds, indicating roughly the same degree of correlation in both compounds. In addition, the estimated Dingle temperature ( $T_D$ ) is roughly the same for all pockets of both compounds. Therefore, we infer that there must be another prevailing cause for the higher  $T_{SDW}$  in  $\text{Eu122}$ .

TABLE I: Comparison between the SdH parameters of Ba122 and Eu122 obtained experimentally and theoretically in this work. Negative effective masses mean hole pockets.

Pocket	BaFe <sub>2</sub> As <sub>2</sub>						EuFe <sub>2</sub> As <sub>2</sub>					
	$F(T)$	$A/A_{BZ}$ (%)	$m^*/m_e^*$	$m_{DFT}^*/m_e^*$	$R$	$T_D$ (K)	$F$ (T)	$A/A_{BZ}$	$m^*/m_e^*$	$m_{DFT}^*/m_e^*$	$R$	$T_D$
$\gamma$	90(10)	0.3	0.7(2)	0.4	2.1	5(2)	60(10)	0.2	1.0(2)	0.4	1.2	-
$\alpha$	430(10)	1.4	1.5(2)	-0.8	2.1	4(1)	340(10)/380(10)	1.3	1.5(2)/1.9(2)	-0.8	1.4	4(1)
$\delta$	510(10)	1.7	-	1.2	0.8	3(1)	580(10)	1.4	-	1.7	0.5	3(1)

TABLE II: Comparison between the SdH frequencies of Ba122 obtained experimentally in refs.<sup>19,20</sup>

Pocket	BaFe <sub>2</sub> As <sub>2</sub> ref. <sup>19</sup>				BaFe <sub>2</sub> As <sub>2</sub> ref. <sup>20</sup>			
	$F(T)$	$A/A_{BZ}$ (%)	$m^*/m_e^*$	$T_D$ (K)	$F$ (T)	$A/A_{BZ}$	$m^*/m_e^*$	$T_D$
$\gamma$	80(10)	0.3	0.7(2)	3(1)	$\sim 90$	-	0.9(1)	-
$\alpha$	440(10)	1.7	1.2(3)	4(1)	$\sim 440$	1.3	2.1(1)	4(1)
$\delta$	-	-	-	-	$\sim 500$	1.4	2.4(3)	3(1)

In order to unveil this matter, we now turn our attention to the angle dependence of the extremal orbits in Eu122 and Ba122 compounds, shown in Fig. 4. Interestingly, the anisotropy of the pockets displays the most contrasting behavior of our study. On one hand, Fig. 4b shows an anisotropic behavior for  $\gamma$ ,  $\beta$  ( $=\gamma$ ) and  $\delta$  pockets in Ba122. The highly eccentric branches  $\gamma$  and  $\beta$  are associated with large quasi-2D cylinders which show the expected  $1/\cos(\theta)$  dependence (solid lines) and ellipticity of  $\sim 5$ . On the other hand, Fig. 4a presents fairly isotropic branches for the  $\gamma$  and  $\delta$  pockets in Eu122. Such isotropy extends over the entire angular range and suggests the presence of largely three-dimensional isotropic FS sections. In addition, the  $\alpha$  (hole) pocket for both compounds displays a weaker angular dependence that cannot be fitted to  $1/\cos(\theta)$ , suggesting that this particular isotropic pocket remains unaltered in the series.

All the above experimental results allow us to conclude that the FS sheets in Ba122 are much more 2D than in Eu122, suggesting that the bidimensional/planar ( $xy$  and/or  $x^2 - y^2$ ) orbital contribution to the Fe 3d bands is higher in BaFe<sub>2</sub>As<sub>2</sub>. In fact, our result is in complete agreement with ARPES measurements in Ba122 and Eu122, which revealed that the hole  $xy$  pocket in Ba122 is half the size of Eu122 due to an increase of the planar  $xy$  occupation in the Ba-rich end<sup>13</sup>. Interestingly, one might expect that the lower dimensionality of Ba122 would favor a higher  $T_{SDW}$ , as compared with Eu122. However, the opposite behavior is found experimentally here and  $T_{SDW}$  is about 50 K lower in Ba122. As the SDW state in these materials is believed to be associated with itinerant Fe 3d bands, it is plausible that an increase in the planar character of the bands could destabilize the 3D itinerant SDW state.

Although we believe that the interpretation of the experimental results is quite consistent, it is desirable to confront the reported data with band structure calculations, when available. A rigorous band structure calculations for EuFe<sub>2</sub>As<sub>2</sub> is not a easy task due to the pres-

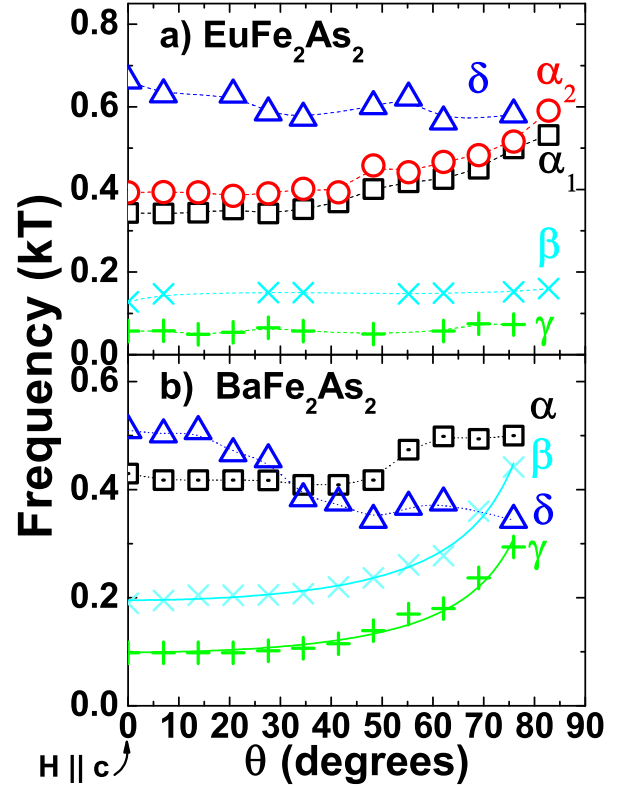


FIG. 4: Angular field dependence (anisotropy) of the observed QO frequencies of a) EuFe<sub>2</sub>As<sub>2</sub> (Eu122) and b) BaFe<sub>2</sub>As<sub>2</sub> (Ba122).

ence of the Eu 4f electrons. However, we will show that a fairly good agreement with the experiments could be obtained by performing band structure calculations for both Ba122 and Eu122 compounds using the LDA+U approach, as detailed in Section II. As usually performed in these materials<sup>17-20</sup>, in order to improve the agreement between the calculated and the measured frequencies, we

have shifted the energies of the  $\alpha$ ,  $\delta$ , and  $\gamma$  bands of Ba122 by + 48 meV, - 54 meV, and +35 meV, respectively, and those of Eu122 by + 41 meV, -54 meV, and -30 meV, respectively. The calculated effective masses,  $m_{DFT}^*$ , also display agreement with the experimental data, as shown in Table I. We note that an ideal quantitative agreement of effective masses is often hindered by the sensitivity of the calculations to the Fermi level and to the magnetic moment.

Nevertheless, although both Fermi surfaces are very similar, a quantitative analysis of the anisotropy can be performed by using the ratio between the extremal areas at  $90^\circ$  and  $0^\circ$ . The extracted values for the anisotropy ratio  $R = F(90^\circ)/F(0^\circ)$  are displayed in Table I. Our results show that all bands in Ba122 have higher  $R$  values than Eu122, confirming that they are more anisotropic. Remarkably, the most prominent difference in anisotropy between Ba122 and Eu122 is observed in the  $\gamma$  pocket, in excellent agreement with our experimental results.

Intriguingly, we also find that the Fermi surfaces in  $\text{EuFe}_2\text{As}_2$  split when the calculations assume that the Eu moments ferromagnetically align with one another. The calculated splitting occurs for all three surfaces, but is significantly more prominent in the  $\alpha$  and  $\delta$  pockets. No such splitting is observed in  $\text{BaFe}_2\text{As}_2$  likely due to the lack of spin moments in the intercalant plane.

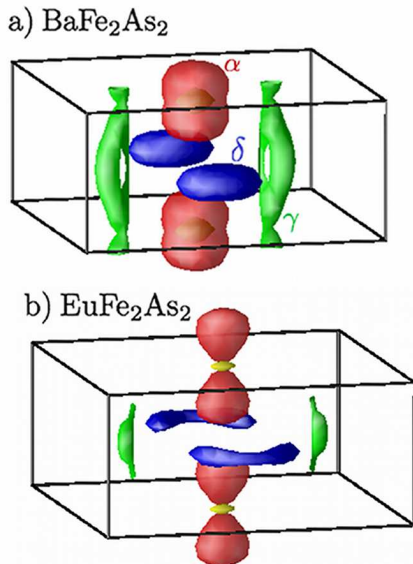


FIG. 5: The shifted Fermi surfaces of a)  $\text{BaFe}_2\text{As}_2$  and b)  $\text{EuFe}_2\text{As}_2$  compounds in the magnetic phase. We identify the large hole sheet (red) as the  $\alpha$  pocket, the crescent electron sheet (blue) as the  $\delta$  pocket, and the tube-like electron pocket (green) as the  $\gamma$  pocket.

In addition, it is worth mentioning that our macro-

scopic understanding about the underlying physics of these materials is in great agreement with the findings from an independent microscopic spin probe technique, namely Electron Spin Resonance (ESR). Recent reported ESR measurements also revealed an increase of both anisotropy and localization of the Fe 3d bands at the FeAs plane in  $\text{Eu}_{1-x}\text{Ba}_x\text{Fe}_2\text{As}_2$  with increasing  $x$  content<sup>29,30</sup>. Moreover, ESR data also pointed to a similar density of states for both under and overdoped  $\text{Ba}_{1-x}\text{Eu}_x\text{Fe}_2\text{As}_2$  compounds.

Enlightened by previous microscopic measurements and calculations, we suggest a plausible scenario for the role of local distortions on the fermiology of Eu122 and Ba122. Previous EXAFS (Extended X-Ray Absorption Fine Structure) measurements on In-grown Ba122 single crystals revealed a decrease of the Fe-As distances as  $T_{SDW}$  is suppressed by either chemical substitution (K and Co) or applied pressure<sup>31</sup>. In addition, DFT+DFMT calculations also predicted a decrease of the planar  $xy$  orbital contribution to the FS as the Fe-As distance is increased<sup>15</sup>. Within this context, our present data combined with microscopic techniques suggest that the As ions are located further away from the Fe plane, i. e. the Fe-As tetrahedra have greater height. In fact, the height of the Fe-As tetrahedra defined as  $z_{As}$  is known to be greater in Eu122 ( $z_{As} = 0.362$ ,<sup>32</sup>) than in Ba122 ( $z_{As} = 0.3545(1)$ ,<sup>2</sup>). Further EXAFS measurements might provide relevant ingredients to this scenario.

In summary, we have observed Shubnikov-de Haas effect by performing high-field electrical resistivity measurements on high quality single crystals of  $\text{EuFe}_2\text{As}_2$  and  $\text{BaFe}_2\text{As}_2$ . Although three low frequency pockets are observed for both compounds with comparable sizes and effective masses, our results show that the electronic structure in Eu122 is much more isotropic and three-dimensional when compared with Ba122, suggesting that all the Fe 3d orbitals contribute evenly to the FS in the Eu-rich extreme. Our main finding sheds new light on the mechanism of the spin-density wave phase suppression which leads to the emergence of unconventional superconductivity in this family of materials.

#### IV. ACKNOWLEDGMENTS

This work was supported by FAPESP-SP, AFOSR MURI, CNPq and FINEP-Brazil. L.B. is supported by DOE-BES through award DE-SC0002613. Work at NHMFL was performed under the auspices of the NSF through the grant NSF-DMR-0084173 and the State of Florida. Funding for M.D.J. was provided by the U.S. Office of Naval Research through the Naval Research Laboratory's Basic Research Program.

<sup>1</sup> Y. Kamihara, T. Watanabe, M. Hirano, and H. Hosono. J. Am.Chem. Soc.**130**, 3296 (2008).

<sup>2</sup> M. Rotter, M. Tegel, I. Schellenberg, W. Hermes, R.



- Pottgen, D. Johrendt. Phys. Rev. B **78**, 020503(R) (2008).
- <sup>3</sup> M. Rotter, M. Tegel, and D. Johrendt. Phys. Rev. Lett. **101** (2008) 107006.
  - <sup>4</sup> C. Wang, L. Li, S. Chi, Z. Zhu, Z. Ren, Y. Li, Y. Wang, X. Lin, Y. Luo, S. Jiang, X. Xu, G. Cao and Z. Xu. EPL, **83** (2008) 67006.
  - <sup>5</sup> K. Ishida, Y. Nakai and H. Hosono, J. Phys. Soc. Japan **78**, 062001 (2009); D. C. Johnston, Adv. Phys. **59**, 803 (2010); J. Paglione and R. L. Greene, Nature Phys. **6**, 645 (2010); P. C. Canfield and S. L. Bud'ko, Annu. Rev. Cond. Mat. Phys. **1**, 27 (2010); H. H. Wen and S. Li, Annu. Rev. Cond. Mat. Phys. **2**, 121 (2011); G. R. Stewart. Rev. Mod. Phys. **83**, 1589-1652 (2011).
  - <sup>6</sup> R. R. Urbano, E. L. Green, W. G. Moulton, A. P. Reyes, P. L. Kuhns, E. M. Bittar, C. Adriano, T. M. Garitezi, L. Bufaiçal, and P. G. Pagliuso. Phys. Rev. Lett., **105** 107001 (2010).
  - <sup>7</sup> T.M. Garitezi, C. Adriano, P. F. S. Rosa, E. M. Bittar, L. Bufaical, R. L. de Almeida, E. Granado, T. Grant, Z. Fisk, M. A. Avila, R. A. Ribeiro, P. L. Kuhns, A. P. Reyes, R. R. Urbano, P. G. Pagliuso. Brazilian Journal of Physics, **43**, 223 (2013).
  - <sup>8</sup> H. S. Jeevan, Z. Hossain, D. Kasinathan, H. Rosner, C. Geibel, and P. Gegenwart. Phys. Rev. B **78**, 052502 (2008).
  - <sup>9</sup> S. Jiang, Y. Luo, Z. Ren, Z. Zhu, C. Wang, X. Xu, Q. Tao, G. Cao and Z. Xu. New J. Phys. **11**, 025007 (2009).
  - <sup>10</sup> B. Zhou, Y. Zhang, L. Yang, M. Xu, C. He, F. Chen, J. Zhao, H. Ou, J. Wei, B. Xie, T. Wu, G. Wu, M. Arita, K. Shimada, H. Namatame, M. Taniguchi, X. H. Chen, and D. L. Feng, Phys. Rev. B **81**, 155124 (2010).
  - <sup>11</sup> D. Graf et al. Phys. Rev. B **85**, 134503 (2012).
  - <sup>12</sup> S. de Jong, E. van Heumen, S. Thirupathaiah, R. Huisman, F. Massee, J. B. Goedkoop, R. Ovsyannikov, J. Fink, H. A. Drr, A. Gloskovskii, H. S. Jeevan, P. Gegenwart, A. Erb, L. Patthey, M. Shi, R. Follath, A. Varykhalov and M. S. Golden. EPL, **89**, 27007 (2010).
  - <sup>13</sup> S. Thirupathaiah. PhD thesis. *Electronic structure studies of ferro-pnictide superconductors and their parent compounds using angle-resolved photoemission spectroscopy (ARPES)*. Berlin, 2011.
  - <sup>14</sup> H. Ding, K. Nakayama, P. Richard, S. Souma, T. Sato, T. Takahashi, M. Neupane, Y.-M. Xu, Z.-H. Pan, A.V. Federov, Z. Wang, X. Dai, Z. Fang, G.F. Chen, J.L. Luo, N.L. Wang. J. Phys. Condens. Matt. **23**, 135701 (2011).
  - <sup>15</sup> Z. P. Hin, K. Haule, and G. Kotliar. Nature Materials **10**, 932-935 (2011).
  - <sup>16</sup> D. Schoenberg. Magnetic Oscillations in Metals. Cambridge University Press, 1984.
  - <sup>17</sup> S. E. Sebastian. Quantum Oscillations in Iron Pnictide Superconductors. Chapter 4 in 'Magnetism and Superconductivity: from Cuprates to Iron-Pnictides'. Published by Pan Stanford.
  - <sup>18</sup> S. E. Sebastian, J. Gillett, N. Harrison, P. H. C. Lau, D. J. Singh, C. H. Mielke and G. G. Lonzarich. J. Phys.: Cond. Matt. **20** 422203 (2008).
  - <sup>19</sup> J. G. Analytis, R. D. McDonald, J. Chu, S. C. Riggs, A. F. Bangura, C. Kucharczyk, M. Johannes, I. R. Fisher. Phys. Rev. B **80**, 064507 (2009).
  - <sup>20</sup> T. Terashima, N. Kurita, M. Tomita, K. Kihou, C. Lee, Y. Tomioka, T. Ito, A. Iyo, H. Eisaki, T. Liang, M. Nakajima, S. Ishida, S. Uchida, H. Harima, and Shinya Uji. Phys. Rev. Lett. **107**, 176402 (2011).
  - <sup>21</sup> N. Harrison, R. D. McDonald, C. H. Mielke, E. D. Bauer, F. Ronning and J. D. Thompson. J. Phys. Condens. Matter **21** 322202 (2009).
  - <sup>22</sup> N. Kurita, M. Kimata, K. Kodama, A. Harada, M. Tomita, H. S. Suzuki, T. Matsumoto, K. Murata, S. Uji and T. Terashima. J. Phys.: Conf. Ser. **273**, 012098 (2011).
  - <sup>23</sup> P. Blaha, K. Schwarz, G.K.H. Madsen, D.Kvasnick and J. Luitz, WIEN2K, An Augmented Plane Wave + Local Orbitals Program for Calculating Crystal Properties (Karlheinz Schwarz, Techn. Universitat Wien, Austria), 2001. ISBN 3-9501031-1-2.
  - <sup>24</sup> J.P. Perdew and Y. Wang, Phys. Rev. B **45**, 13244 (1992)
  - <sup>25</sup> V.I. Anisimov, J. Zaanen and O.K. Andersen, Phys. Rev. B **44**, 943 (1991)
  - <sup>26</sup> Y. Xiao, Y. Su, M. Meven, R. Mittal, C. M. N. Kumar, T. Chatterji, S. Price, J. Persson, N. Kumar, S. K. Dhar, A. Thamizhavel, and Th. Brueckel, Phys. Rev. B **80**, 174424 (2009)
  - <sup>27</sup> Q. Huang, Y. Qiu, Wei Bao, M. A. Green, J. W. Lynn, Y. C. Gasparovic, T. Wu, G. Wu, and X. H. Chen. PRL **101**, 257003 (2008).
  - <sup>28</sup> Y. Xiao *et al.* Phys. Rev. B **81**, 220406(R) (2010).
  - <sup>29</sup> P. F. S. Rosa, C. Adriano, W. Iwamoto, T. M. Garitezi, T. Grant, Z. Fisk, and P. G. Pagliuso. Phys. Rev. B **86**, 165131 (2012).
  - <sup>30</sup> P. F. S. Rosa, C. Adriano, T. M. Garitezi, T. Grant, Z. Fisk, R. R. Urbano, and P. G. Pagliuso. Sci. Rep. **4**, 6543 (2014).
  - <sup>31</sup> E. Granado, L. Mendonca-Ferreira, F. Garcia, G. de M. Azevedo, G. Fabbri, E. M. Bittar, C. Adriano, T. M. Garitezi, P. F. S. Rosa, L. F. Bufaical, M. A. Avila, H. Terashita, and P. G. Pagliuso. Phys. Rev. B **83**, 184508 (2011).
  - <sup>32</sup> H. Raffius, E. Morsen, B. D. Mosel, W. Muller, W. Warmuth, W. Jeitschko, L. Terbuchte and T. J. Vomhof. J. Phys. Chem. Solids **54**, 135 (1993).